Dyson, H. J., Lerner, R. A., & Wright, P. E. (1988) *Annu. Rev. Biophys. Chem. 17*, 305-324.
Jacob, C. O., Sela, M., & Arnon R. (1983) *Proc. Natl. Acad. Sci. U.S.A. 80*, 7611-7615.
Levy, R., Assulin, O., Scherf, T., Levitt, M., & Anglister, J. (1989) *Biochemistry 28*, 7168-7175.
Pedoussaut, S., Delmas, A., Milhaud, G., Rivaille, P., & Grauz-Guyon, A. (1989) *Mol. Immunol. 26*, 115-119.
Steward, M. W., & Howard, C. R. (1987) *Immunol. Today 8*, 51-58.
Van Regenmortel, M. H. V. (1987) *Trends Biochem. Sci. 12*, 237-240.

Crystal Structure of Two Covalent Nucleoside Derivatives of Ribonuclease A[†,‡]

Joseph Nachman,[§,∥] Maria Miller,[§] Gary L. Gilliland,[⊥] Robert Carty,[#] Matthew Pincus,[○] and Alexander Wlodawer*[,§]

Crystallography Laboratory, BRI-Basic Research Program, NCI-Frederick Cancer Research Facility, P.O. Box B, Frederick, Maryland 21701, Center for Advanced Research in Biotechnology, 9600 Gudelsky Drive, Rockville, Maryland 20850, Center for Chemical Technology, National Institute of Standards and Technology, Gaithersburg, Maryland 20899, Department of Biochemistry, State University of New York, Health Science Center at Brooklyn, 450 Clarkson Avenue, Brooklyn, New York 11203-2098, and Department of Pathology, State University of New York, Health Science Center at Syracuse, 750 East Adams Street, Syracuse, New York 13210

Received June 8, 1989; Revised Manuscript Received September 14, 1989

ABSTRACT: Crystal structures of two forms of ribonuclease A with deoxynucleosides covalently bound to respectively His12 and His119 have been solved. One form, T-H12-RNase, has a deoxythymidine bound to N_{ϵ_2} of His12, while the other one, U-H119-RNase, has a deoxyuridine bound to N_{δ_1} of His119. The two crystal forms are nearly isomorphous, with two molecules in the asymmetric unit. However, the modified ribonucleases differ both in their enzymatic activities and in the conformation of the catalytic site and of the deoxynucleoside–histidine moiety. T-H12-RNase is characterized by complete loss of enzymatic activity; in this form the deoxynucleoside completely blocks the catalytic site and forms intramolecular contacts with residues associated with both the B1 and B2 sites. U-H119-RNase retains 1% of the activity of the unmodified enzyme, and in this form His119 adopts a different orientation, corresponding to the alternate conformation reported for this residue; the deoxynucleoside–histidine moiety points out of the active site and does not form any contacts with the rest of the protein, thus allowing partial access to the catalytic site. On the basis of these structures, we propose possible mechanisms for the reactions of bromoacetamido nucleosides with ribonuclease A.

We report here the X-ray structures of two modified forms of bovine pancreatic ribonuclease A (RNase A),[1] with deoxynucleosides covalently bound to respectively His12 and His119. These two histidine residues, together with Lys41, form the catalytic site of RNase A. This study continues the already large body of crystallographic studies of this enzyme and of its complexes with various inhibitors, performed in order to understand the details of the mechanism of reaction catalyzed by RNase A [see review by Wlodawer (1985) and references cited therein; Campbell & Petsko, 1987; Wlodawer et al., 1988].

RNase A reacts rapidly with a variety of bromoacetamido pyrimidine nucleosides to form covalent derivatives in which either His12 or His119 is alkylated (Hummel et al., 1987). 3′-(Bromoacetamido)-3′-deoxythymidine forms four derivatives; the major product is [N^{ϵ_2}-[[[(3′-deoxy-3′-thymidinyl)-amino]carbonyl]methyl]histidine-12]ribonuclease A (T-H12-RNase) and is enzymatically inactive. However, T-H12-RNase can react further with the nucleoside alkylating agent to produce a disubstituted derivative in which both His12 and His119 are alkylated. The production of a disubstituted derivative suggests that the nucleoside moiety in the monosubstituted derivative binds at more than one site with only partial occupancy of the B_1–R_1–p_1 site or that the nucleoside exhibits conformational flexibility which limits residency time in the active site. These two alternatives may be distinguished by examining the high-resolution X-ray crystal structure of T-H12-RNase. Alternate binding sites may exist for the deoxythymidinyl moiety in T-H12-RNase, one of which permits further binding of bromoacetamido nucleoside and subsequent alkylation of His119. Alternatively, the deoxythymidinyl residue may be highly mobile, in which case the structure would appear disordered.

3′-(Bromoacetamido)-3′-deoxyuridine alkylates RNase A only at His119 and produces three major derivatives. The product formed in highest yield is [N^{δ_1}-[[[(3′-deoxy-3′-uridinyl)amino]carbonyl]methyl]histidine-119]ribonuclease

[†] This research was sponsored in part by the National Cancer Institute, DHHS, under Contract N01-C0-74101 with BRI.

[‡] Crystallographic coordinates have been submitted to the Brookhaven Protein Data Bank.

* Corresponding author.
[§] NCI-Frederick Cancer Research Facility.
[∥] Present address: Biotechnology Research Institute, National Research Council of Canada, 6100 Royalmount Ave., Montreal, Quebec H4P 2R2, Canada.
[⊥] Center for Advanced Research in Biotechnology and National Institute of Standards and Technology.
[#] Health Science Center at Brooklyn.
[○] Health Science Center at Syracuse.

[1] Abbreviations: RNase A, ribonuclease A; T-H12-RNase, [N^{ϵ_2}-[[[(3′-deoxy-3′-thymidinyl)amino]carbonyl]methyl]histidine-12]ribonuclease A; U-H119-RNase, [N^{δ_1}-[[[(3′-deoxy-3′-uridinyl)amino]-carbonyl]methyl]histidine-119]ribonuclease A.

0006-2960/90/0429-928$02.50/0

A (U-H119-RNase), and it exhibits 1% of the activity of unmodified RNase A in hydrolytic and transphosphorylation assays (Hummel et al., 1987). Smaller amounts of the His119 N_{ϵ_2} derivative exhibiting 5% residual enzymatic activity are also observed, as well as a disubstituted derivative in which both side-chain imidazole N atoms of His119 are modified.

In this paper, we describe the crystal structures of T-H12-RNase and U-H119-RNase at 1.8-Å resolution. We have focused on understanding the contribution of His119 side-chain flexibility (Borkakoti et al., 1982) to the catalytic mechanism and on explaining the observed reactions between the nucleosides and the active site histidines in the enzyme.

Experimental Procedures

(*a*) *Preparation of the Enzyme.* RNase A was alkylated with 3′-(bromoacetamido)-3′-deoxythymidine and 3′-(bromoacetamido)-3′-deoxyuridine according to previously described procedures (Hummel et al., 1987). Reaction mixtures were purified by chromatography on preparative columns of Amberlite CG-50, type III, ~400 mesh (Pincus et al., 1975; Carty & Hirs, 1968). Further purification was achieved by ion exchange chromatography on CM-52 (Lin et al., 1984). Purified proteins were desalted by passage over Sephadex G-25 columns in 0.1 M acetic acid and were lyophilized.

(*b*) *Crystallization and Data Collection.* T-H12-RNase was crystallized from a 28% ammonium sulfate solution containing 25–30 mg/mL enzyme and 3 M CsCl; the pH was adjusted to 5.1 with acetate buffer. Prior to data collection a crystal was soaked for about 1 h in an 80% solution of ammonium sulfate, in order to wash out the CsCl, and then was mounted in a capillary. The crystallographic parameters of T-H12-RNase crystals were established from precession photographs. It was found that they belong to space group $P2_12_12_1$ with a = 53.14, b = 64.61, and c = 73.64 Å and two molecules per asymmetric unit.

Diffraction data extending to 1.77-Å resolution were collected with a Siemens imaging proportional counter (IPC), an electronic area detector, mounted on a Supper oscillation camera controlled by a Cadmus 9000 computer. The X-ray source used to generate Cu Kα radiation was an Elliott-GX-21 rotating anode, operating at 70 mA, 40 kV, with a 0.3 × 0.3 mm focal spot and a 0.3-mm collimator. Monochromatization was provided by a Huber graphite monochromator. All data were collected from one crystal at well-controlled room temperature (16–18 °C). The detector angle was set at 26°, and the crystal-to-detector distance was set at 10 cm. The data frames or electronic images consisted of the diffraction data from a 0.25° oscillation of the crystal, counted for 110 s each. The individual data frames were contiguous in that the beginning of each small oscillation range coincided with the end of the previous range. Approximately 400 data frames, corresponding to 100° of crystal rotation, were recorded for each of three crystal orientations. The crystal was repositioned in the X-ray beam by adjustment of the goniometer arcs and the x, y, and z translations.

The determination of crystal orientation and the integration of reflection intensities were performed with the XENGEN program system (Howard et al., 1987). There were 60 943 observations of 21 460 unique reflections of the 22 820 possible at 1.77 Å. The data scaled with a weighted least-squares R factor on intensity of 0.037; 17 494 of the measured unique reflections had significant intensity [$I > 1.5\sigma(I)$].

U-H119-RNase was crystallized under conditions very similar to those of T-H12-RNase, and the crystals were treated in the same way prior to data collection. The crystals of U-H119-RNase are nearly isomorphous with those of T-H12-RNase with cell dimensions of a = 52.75, b = 64.10, and c = 73.15 Å.

Five crystals of U-H119-RNase were used for data collection. Data for one crystal were measured with a Siemens IPC mounted on a Huber diffractometer, with X-rays generated by a Phillips 3100 sealed-tube generator operated at 40 kV, 44 mA. The detector angle was set at 20°, and the crystal-to-detector distance was 10 cm. Data for the other four crystals were collected on a Siemens IPC mounted on a three-axis camera. X-rays were provided by a Rigaku RU-200 rotating-anode generator operated at 50 kV, 100 mA, with a 0.3-mm focal spot. The detector-to-crystal distance was set at 10 cm, while the detector angle was varied between 0° and 27°. The total number of reflections used for scaling was 162 247, resulting in 19 632 unique reflections with R_{sym} = 0.078. The total number of observed reflections [$I > 1.5\sigma(I)$] with 17 615, and the final data set was virtually complete to 2-Å resolution, while only about half of the data in the 1.8–2-Å shell were measured.

(*c*) *Structure Solution.* The structure of T-H12-RNase was solved by molecular replacement techniques, as implemented in the program package MERLOT (Fitzgerald, 1988). The orientation of the two molecules in the asymmetric unit was found by performing Crowther's fast-rotation function (Crowther, 1972), on a search grid of 2.5° in α and 5° in β and γ (where α, β, and γ are Euler angles), and by use of data between 8.0 and 3.0 Å. The search model was the structure of ribonuclease A refined at 1.26-Å resolution (Wlodawer et al., 1988), from which solvent molecules and hydrogen atoms were eliminated. The search yielded a very clean correlation map, with two virtually equal maxima at 6.0 and 5.9 rms units above background (corresponding to respectively 100% and 98% of the maximum peak height) and no other peaks above 75%. The two molecules in the asymmetric unit are related by an approximate 2-fold rotation about an axis inclined by 118° with respect to the y axis and whose projection onto the xy plane makes an angle of 65° with the x axis.

The positions of the two molecules were found by using the translation function of Crowther and Blow (1967), which searches both for the vectors between symmetrically independent molecules and for vectors between each independent molecule and its symmetry equivalents; one search for each vector was performed. The trial model was built by rotating the model used in the orientation search through the two sets of Euler angles, which yielded the best solution for the rotation function, i.e., presumably the correct orientations of the two molecules. All searches yielded very clear maps, with no peaks higher than 75% of the maximum peak height; the intensity of the highest peak in the search for the vector between the two independent molecules was 8.5 rms units. The maxima of these maps formed seven mutually consistent sets of intermolecular vectors, yielding the positions of the two molecules.

Finally, the rotational and translational parameters were optimized by an R factor minimization procedure (Ward et al., 1975). After three cycles of minimization the R factor for data between 8.0- and 3.2-Å resolution dropped from 0.498 to 0.456. However, the changes in the parameters were minimal: 1° in the orientation of the molecules and 0.01 fractions of unit-cell edge (i.e., less than 1 Å) in the translational parameters.

(*d*) *Structure Refinement.* The coordinates resulting from the previous step were refined with the modified restrained least-squares refinement program PROLSQ (Hendrickson, 1985). The version of the program used for these studies

Table I: Summary of the Refinement of T-H12-RNase

cycle no.	resolution (Å)	*R* factor	observations
0	10.0–3	0.45	after molecular replacement
11	10.0–3	0.287	overall *B* factor; distance restraints between the two molecules in the asymmetric unit; $F_o - F_c$ and $2F_o - F_c$ maps calculated; side chains refitted; solvent molecules added; positive $F_o - F_c$ density near N_{ϵ_2} of His12
56	10.0–1.8	0.192	individual *B* factors; no distance restraints between the two molecules in the asymmetric unit; His119 refitted to position corresponding to its alternative conformation; clear $F_o - F_c$ density for deoxythymidine (Figure 1)
104	10.0–1.8	0.162	highest peak in $F_o - F_c$ map: 3.75σ

incorporates a fast Fourier algorithm to speed up calculations (Finzel, 1987), and it restrains intermolecular contacts (Sheriff, 1987). Progress of refinement is summarized in Table I. Eleven cycles of refinement using 10.0–3.0-Å resolution data, with an overall temperature factor, and applying distance restraints between the two molecules in the asymmetric unit lowered the *R* factor from 0.45 to 0.287. At this stage both a $2F_o - F_c$ map and a $F_o - F_c$ map were calculated, on the basis of which the side chains of some of the residues were refitted and some solvent molecules (treated as waters) were added. The $F_o - F_c$ map revealed a strong, large positive peak near atom N_{ϵ_2} of His12, the attachment site of the deoxythymidine.

During the next four stages of refinement, totaling 45 cycles, all data extending to 1.8-Å resolution were gradually added, individual isotropic temperature factors were introduced, and finally, the restraints linking the coordinates of the two molecules in the asymmetric unit were eliminated. After each stage difference maps were calculated, solvent molecules were added, and where necessary, side chains were refitted. The most important change with respect to the starting model is that the other histidine residue in the active site, His119, had to be completely refitted into a position corresponding to its alternative conformation reported in other crystallographic studies (Borkakoti et al., 1982, 1983; Borkakoti, 1983). At this point the *R* factor was 0.192, and the difference Fourier map revealed density for the acetamido group linking the deoxythymidine to N_{ϵ_2} of His12. A new fragment $F_o - F_c$ map was calculated after all solvent molecules in the active site were removed, as well as the acetamido link, and it provided a very clear density into which the whole of the substituent was then fitted. The structure thus obtained was further refined in six stages for a total of 48 cycles, until no further improvement could be observed. The electron density for His12 and the deoxythymidine is shown in Figure 1.

The final model contains 248 protein residues, 2 deoxythymidine groups (i.e., 2 RNase molecules with 124 residues and 1 substituent each), and 246 solvent molecules per asymmetric unit (Figure 2A). The $F_o - F_c$ difference Fourier map calculated on the basis of this model has no peaks higher than 3.75σ, and none of these peaks can be interpreted as additional solvents. The crystallographic *R* factor is 0.162, the deviations of distances from ideality are 0.016 Å for bond lengths and 0.035 Å for angle distances, and the deviation of chiral volumes from ideality is 0.153 Å^3.

U-H119-RNase was refined in the same way as T-H12-RNase. The refinement started from the atomic coordinates of the T-H12-RNase, partially refined for 56 cycles to an *R* factor of 0.192 (see Table I): no solvent peaks were included in the starting model. Eleven cycles of refinement using data between 10.0- and 2.0-Å resolution lowered the *R* factor from

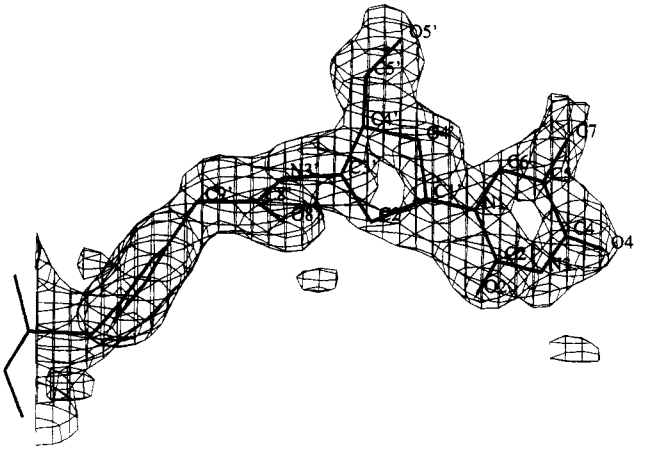

FIGURE 1: Electron density map and the fitted model of the deoxythymidine bound to His12 in molecule II of T-H12-RNase. This map was calculated with the coefficients $|2F_o - F_c|\alpha_c$ and is contoured at the 0.85σ level. The atoms in the nucleoside are shown in the plot.

0.327 to 0.237. The $F_o - F_c$ map calculated at this stage revealed that the side chain of His119, to which the deoxyuridine is bound, has to be refitted into a position corresponding to the conformation of this residue in the native form of RNase (Wlodawer et al., 1988). After 49 more cycles, during which data extending to 1.8 Å were added, the *R* factor was further lowered to 0.202. The $F_o - F_c$ map showed very clear density for the acetamido linking group and for part of the sugar moiety but no density for the pyrimidine ring. The substituent was fitted into this density with an arbitrary orientation of the pyrimidine with respect to the sugar ring and with the sugar pucker chosen to be the same as in the deoxythymidine in the structure of T-H12-RNase (in view of the poor quality of the density for the sugar, this choice is rather arbitrary). The resulting structure was refined for 35 additional cycles. The final model contains 248 protein residues, 2 deoxyuridines, and 181 solvent molecules per asymmetric unit (Figure 2B). The *R* factor is 0.196, and the deviations from ideality are 0.016 Å for bond lengths, 0.031 Å for angle distances, and 0.166 Å^3 for chiral volumes.

RESULTS

(*a*) *Electron Density.* The electron density maps for T-H12-RNase are of very good quality, and refitting of the model was achieved without difficulty. As mentioned in the last section, very clear density could be seen for the new position of the side chain of residue His119 and for the deoxythymidine substituent (Figure 1).

There was practically no density for the amino-terminal residue, Lys1, in molecule I in the asymmetric unit and for the side chain of Lys91 in molecule II; repeated attempts to fit these residues to small peaks in the $F_o - F_c$ difference map were unsuccessful. Excellent density, however, was observed for the corresponding residues in molecule II and molecule I, respectively, although their temperature factors are relatively high. This behavior is a consequence of crystal packing, which causes the two molecules in the asymmetric unit to be in different crystallographic environments. As can be seen in Table IIB, Lys1 in T-H12-RNase II and Lys91 in T-H12-RNase I are involved in direct intermolecular contacts with main-chain carbonyl oxygens of symmetry-related molecules; however, Lys1 in molecule I and Lys91 in molecule II do not participate in such interactions.

No $2F_o - F_c$ density was visible for parts of the side chains of Arg39, Lys66, and Lys104 in T-H12-RNase II, and the corresponding side chains in T-H12-RNase I are also largely

Table II: Intermolecular Contacts in T-H12-RNase

(A) Between the Two Molecules in the Same Asymmetric Unit

molecule I		molecule II		
residue	atom	residue	atom	distance (Å)
Asn62	O	Gly88	N	3.00
Ala64	O	Arg85	NH1	2.75
Ala64	N	Glu86	O	2.83
Arg85	NH1	Ala64	O	2.87
Arg85	NH1	Asp121	OD2	2.90
Arg85	NH2	Asp121	OD2	3.20
Glu86	O	Ala64	N	2.98
Gly88	N	Asn62	O	3.24
Lys104	NZ	Val124	O	3.38
Asp121	OD2	Arg85	NH1	2.86
Asp121	OD2	Arg85	NH2	2.99
Val124	O	Lys104	NZ	3.25

(B) Between Molecules Related by Crystallographic Symmetry[a]

molecule	residue	atom	molecule	residue	atom	distance (Å)
1	Lys91	NZ	*1	Tyr115	O	2.51
2	Lys1	NZ	*2	Ala20	O	3.29
2	Lys1	NZ	*2	Ser21	O	3.40
1	Glu9	OE1	*2	Thr70	OG1	3.46
1	Glu9	OE2	*2	Thr70	OG1	3.28
1	Glu9	OE2	*2	Thr70	N	3.19
1	Ser23	N	*2	Asp38	O	3.15
1	Gln69	OE1	*2	Tyr76	O	3.59
1	Gln69	NE2	*2	Ser77	OG	3.13
1	Tyr76	O	*2	Asn34	ND2	3.55
1	Ser77	OG	*2	Ser32	O	3.46
1	Ser77	OG	*2	Asn34	OD1	3.17
1	Glu111	OE1	*2	Ser77	OG	2.49
2	Tyr76	O	*1	Gln69	OE1	3.59

[a] Symmetry elements vary for different pairs.

disordered; nevertheless, it was possible to fit these side chains to the small peaks in the $F_o - F_c$ and $2F_o - F_c$ maps. The side chain of Gln28 in T-H12-RNase II can be modeled in two distinct conformations, but no density indicating multiple side-chain conformations could be observed for Gln28 in T-H12-RNase I.

The maps for U-H119-RNase are noisier than those of T-H12-RNase, but they do not present any additional problems, except for the lack of density for the pyrimidine ring of deoxyuridine. The density for His119 was very clear throughout the course of the refinement.

(*b*) *Atomic Coordinates.* The peptide backbone and active site residues of the final models of T-H12-RNase and U-H119-RNase including the covalently bound deoxynucleoside are presented in Figure 2. The relationship between the two molecules in the asymmetric unit is similar to that between one of the molecules in the asymmetric unit of ribonuclease B and its symmetry mate by the crystallographic 2_1 screw axis (Williams et al., 1987). After superposition of C_α coordinates, the rms differences between all main-chain atoms in RNase A and the two molecules of T-H12-RNase in the asymmetric unit are 0.502 and 0.504 Å, respectively. For all the side-chain atoms, the deviations are 1.535 and 1.307 Å. The rms difference between each of the molecules of T-H12-RNase and RNase A is plotted in Figure 3B,C.

There are 38 residues in molecule I of T-H12-RNase and 39 in molecule II that have atomic positions with rms deviations from the native RNase larger than 1.0 Å. The largest differences (more than 3.0 Å) between the substituted and native forms of RNase are at residues Lys1, Gln28, Gln69, Arg85, Gln101, Lys104, and His119 in molecules I and II and Lys41 in molecule I only. Residue Lys1 is not very well-defined while His119 adopts the alternate conformation reported by other investigators (Borkakoti et al., 1982, 1983; Borkakoti, 1983). Gln69, Arg85, and Lys104 are involved in intermolecular contacts, both directly and via solvent bridges (see Tables II and III and Section d under Results). In RNase A, these residues do not participate in intermolecular contacts, while multiple side-chain conformations have been reported for Arg85 and Lys104 (Svensson et al., 1987; Wlodawer et al., 1988).

Table III: Solvent Bridges in T-H12-RNase

solvent	atom	molecule	residue	atom	distance (Å)
Wat1001	O	1	Lys104	NZ	2.23
		2	Lys104	NZ	2.69
		1	Ser123	O	3.23
		2	Ser123	O	3.39
Wat1002	O	1	Lys66	NZ	2.81
		2	Lys66	NZ	3.40
Wat1402	O	1	Arg39	NH1	3.22
		2	Lys66	O	2.91
Wat1702	O	2	Arg39	NH1	3.36
		1	Lys66	O	3.34

The large deviation observed for Lys41 in molecule I can be associated with the somewhat higher degree of disorder in the catalytic site of this molecule (see next section), although the corresponding *B* factors are only slightly higher than those in molecule II. Gln28 and Gln101 do not participate in intermolecular contacts in either T-H12-RNase or native RNase, so no explanation based on crystal packing arguments can be provided for the rms deviations of these residues. However, Gln101 was modeled in multiple conformations in RNase A (Svensson et al., 1987; Wlodawer et al., 1988), while no evidence of a multiple conformation for Gln101 was found in the present structure.

Although the rms deviations for the atomic positions of Asp38, Arg39, Lys66, and Asn67 are less than 3.0 Å, they are the only residues whose C_α atoms deviate by more than 1.0 Å from their positions in RNase; the largest deviation is that for C_α for Asp38: 1.384 and 1.592 Å for molecules I and II, respectively. These discrepancies are also a result of different intermolecular contacts in T-H12-RNase and RNase: Asp38 forms direct intermolecular contacts in both the native and substituted form of RNase, but to different residues. In T-H12-RNase, Lys66 forms an intermolecular solvent bridge (see Table III), while in RNase it forms only intramolecular contacts; Asn67 is intimately involved in contacts with the deoxythymidine in T-H12-RNase (see Section c under Results) but has no detectable interactions with other protein or solvent atoms in RNase A (Wlodawer et al., 1988).

The rms deviation between the main-chain atoms of the two molecules of T-H12-RNase in the asymmetric unit is 0.298 Å, while that of the side-chain atoms is 0.796 Å. These differences are significantly smaller than those between each molecule of T-H12-RNase and RNase, indicating that the two T-H12-RNase molecules adopt essentially the same conformation. Indeed, only 16 residues deviate by more than 1.0 Å between the two molecules, out of which 10 are involved in intermolecular contacts. The rms differences between the two molecules are plotted in Figure 3A.

The deviations between the two molecules of U-H119-RNase are similar to those observed for T-H12-RNase (Figure 4A), and the differences with RNase A are also quite similar (Figure 4B,C). These differences clearly exceed the experimental errors present in these structures and are significant.

(*c*) *Deoxythymidine Substituent and Active Site.* In the final model of T-H12-RNase the torsion angle about the glycosidic bond of each deoxythymidine is −168°; i.e., the base is in the anti conformation, similar to that found in A-DNA (Saenger, 1973); the ring pucker is C2′-exo. The temperature

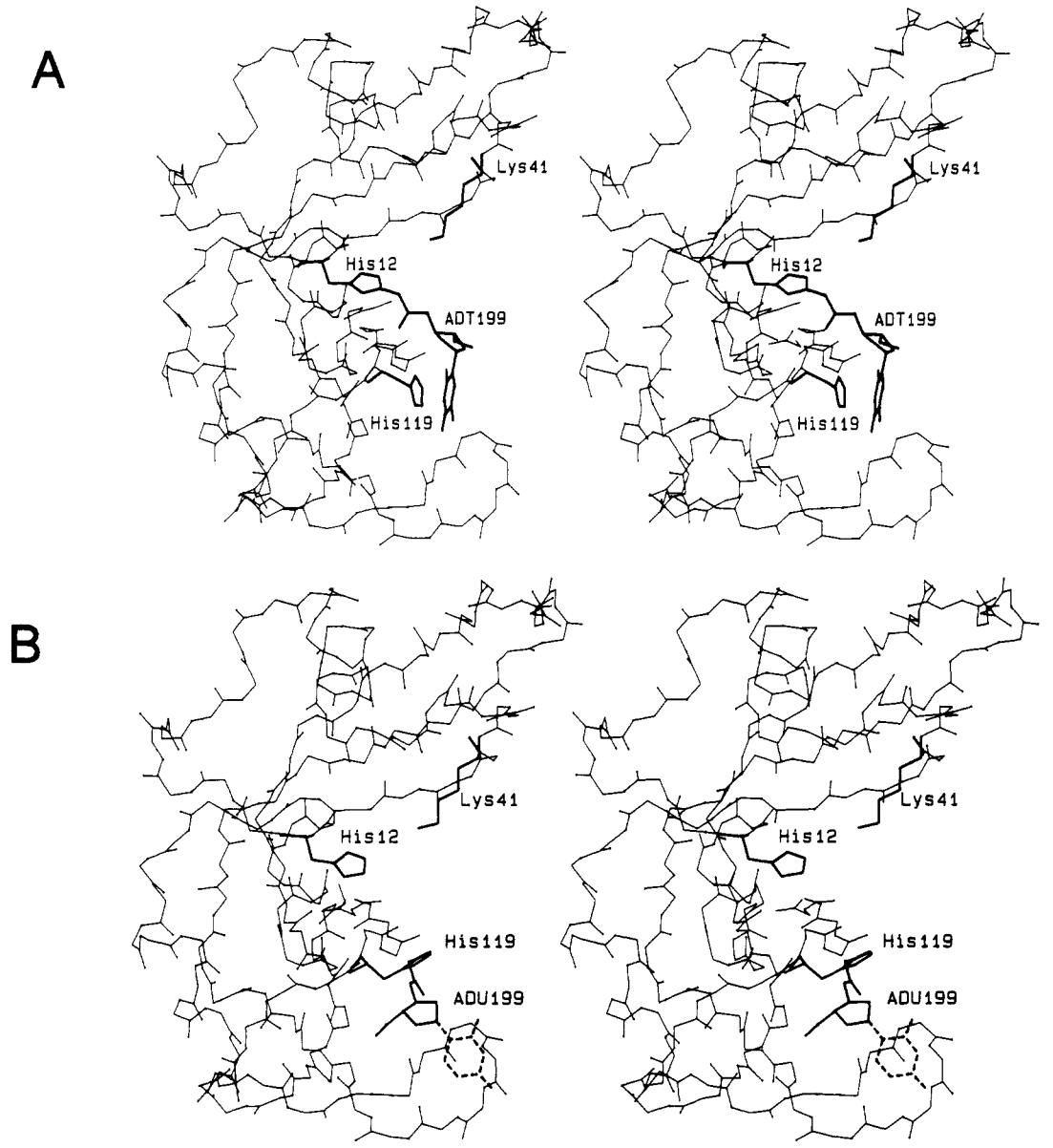

FIGURE 2: Atomic models of the structures discussed: (A) All main-chain atoms of T-H12-RNase I, the side chains of the residues in the active site, and the deoxythymidine group, marked as ADT199; (B) similar model for U-H119-RNase I, with deoxyuridine denoted ADU199. Parts of the structure that were model built without reference to electron density are shown in dashed lines.

factors are unevenly distributed along the substituent; however, they appear correlated with the distances between the atoms of the substituent and His12, ranging from about 10 Å^2 for the aminoacyl link region (comparable to those of the ring atoms of His12, to which it is bonded) to about 40 Å^2 for the pyrimidine ring. This behavior may be interpreted in terms of partial disorder in which the substituent adopts one major conformation, represented in the current model, and a number of minor conformations. The disorder is associated mainly with the rotation around the N3′–C3′ bond and around the glycosidic bond, and possibly with slight variations in the sugar ring pucker. This assumption is partly borne out by the presence of a relatively strong peak in the difference map, forming close contacts with the deoxythymidine residue in one of the molecules in the asymmetric unit. It is also interesting to notice that in molecule I the temperature factors of the substituent and of the solvent molecules in the active site are higher than those in molecule II.

In the structure presented here the deoxythymidine does not specifically occupy any of the parts of the active site traditionally associated with the substrate (i.e. p1, R1–B1, or R2–B2); this is a major departure from the structures of noncovalent complexes between RNase and mono- and dinucleotides reported so far. Rather, it forms contacts with residues associated with all sites (see Table IV): O8′ forms a short hydrogen bond to the N of Phe120, a residue whose side chain is generally associated with site R1–B1 (Richards & Wyckoff, 1973); N3 is hydrogen bonded to O_{δ_1} of Asp121, which is not specifically associated with either R1–B1 or R2–B2 [although, according to Richards and Wyckoff (1973), it is accepted to be part of the active site], and O4 forms a long hydrogen bond to N_{δ_2} of Asn 67, which is part of B2. Out

Table IV: Deoxythmidine Contacts with Active Site Residues and Water Molecules in T-H12-RNase

deoxy-thymidine atom	active site		distance (Å)	
	residue	atom	molecule I	molecule II
O8′	Phe120	N	2.62	2.61
N3	Asp121	OD1	2.79	2.76
O4	Asn67	ND2	3.33	3.31
O4	Wat1399	O	3.16	2.85

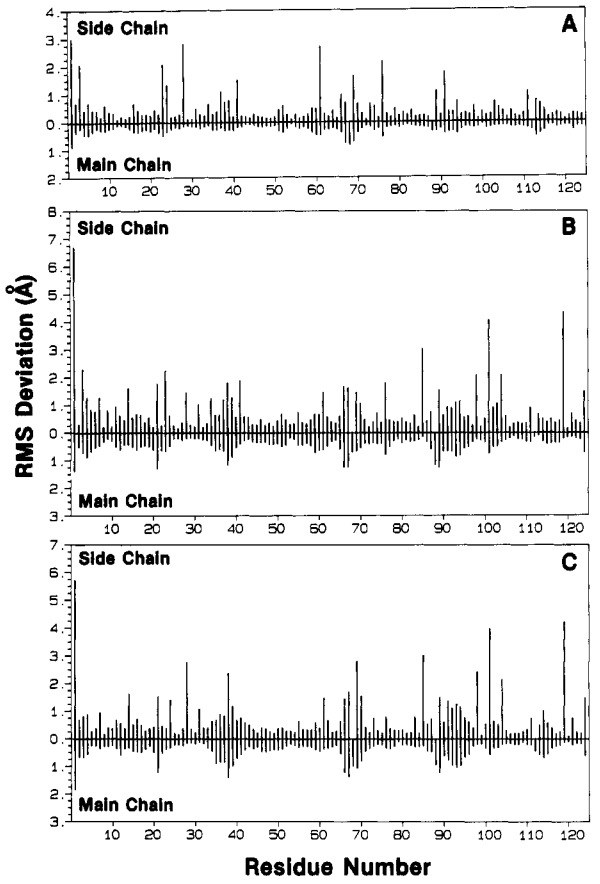

FIGURE 3: Comparison of atomic coordinates for RNase and T-H12-RNase. Data for the main-chain atoms are below and for the side chain atoms are above the central line. (A) rms deviation between the two crystallographically independent molecules of T-H12-RNase; (B) comparison of T-H12-RNase I and RNase A; (C) comparison of T-H12-RNase II and RNase A.

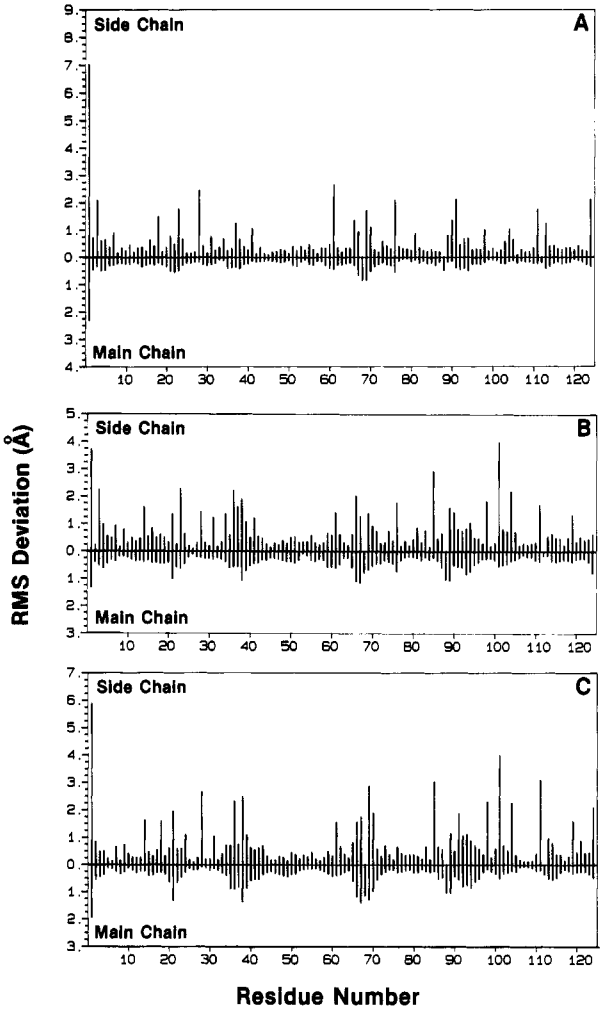

FIGURE 4: Comparison of atomic coordinates for RNase and U-H119-RNase. Data for the main-chain atoms are below and for the side chain atoms are above the central line. (A) rms deviation between the two crystallographically independent molecules of U-H119-RNase; (B) comparison of U-H119-RNase I and RNase A; (C) comparison of U-H119-RNase II and RNase A.

of these, only the hydrogen bond between O8′ and the N of Phe120 is a typical RNase–substrate contact, since O8′ occupies the same region as one of the phosphate oxygens in crystals of RNase A and of RNase–substrate complexes (Richards & Wyckoff, 1973; Wlodawer & Sjölin, 1983). In addition to these direct hydrogen bonds, O4 of deoxythymidine is hydrogen bonded to a water molecule, which in turn forms hydrogen bonds to O_{δ_1} of Asn71, as well as to N_{ϵ_2} of Gln69 in molecule I and to N_{δ_2} of Asn67 in molecule II (see Figure 5A). The temperature factor of this water in T-H12-RNase I is about twice as high as that of the corresponding water in T-H12-RNase II (40.2 vs 19.5 Å), meaning that its position in molecule I is much less well defined than that in molecule II; therefore, the fact that this water molecule does not form identical hydrogen bonds in the two molecules in the asymmetric unit is less important than the fact that it bridges between the base of deoxythymidine and the side chains of residues forming site B2.

Although the density for the deoxyuridine in U-H119-RNase is strongly indicative of a high degree of disorder associated with rotation around the N3′–C3′ bond and, especially, around the glycosidic bond, there is little doubt about the general orientation of the substituent and the conformation of the active site (Figure 5B). As shown in Figure 2, the orientation of the covalently bound deoxynucleosides is completely different in the two substituted forms of RNase: in U-H119 RNase, the deoxyuridine is oriented so that the glycosidic bond and the pyrimidine point out of the active site. It does not form any intramolecular contacts and, possibly, only one intermolecular contact. This might explain the high degree of disorder of the deoxyuridine, since there is apparently nothing to prevent rotation around the N3′–C3′ bond and around the glycosidic bond.

(d) Crystal Packing and Intermolecular Interactions. The crystal packing of the molecules of T-H12-RNase is different than that for the native RNase. Pairs of crystallographically independent molecules pack along the *x* axis, forming long solvent channels. The lists of intermolecular contacts and solvent bridges are given in Tables II and III. The two molecules present in the asymmetric unit are held together by 12 intermolecular hydrogen bonds and by 4 solvent bridges. The differences in distances between equivalent pairs of atoms in the two independent molecules reflect the slight differences in the conformation of the two molecules. Symmetry-related molecules form 10 intermolecular hydrogen bonds and an extensive network of solvent bridges. This is markedly different from the crystal packing of RNase A (Wlodawer & Sjölin, 1983) where only four direct contacts were observed.

As shown in Table IIB, the two molecules in the asymmetric unit are found in different crystallographic surroundings. There is only one contact between molecule I and its symmetry mate and only two between molecule II and its symmetry mate. The rest of the intermolecular hydrogen bonds are between one molecule in the asymmetric unit and the symmetry mate of the other one, and they are different for each of them; i.e.,

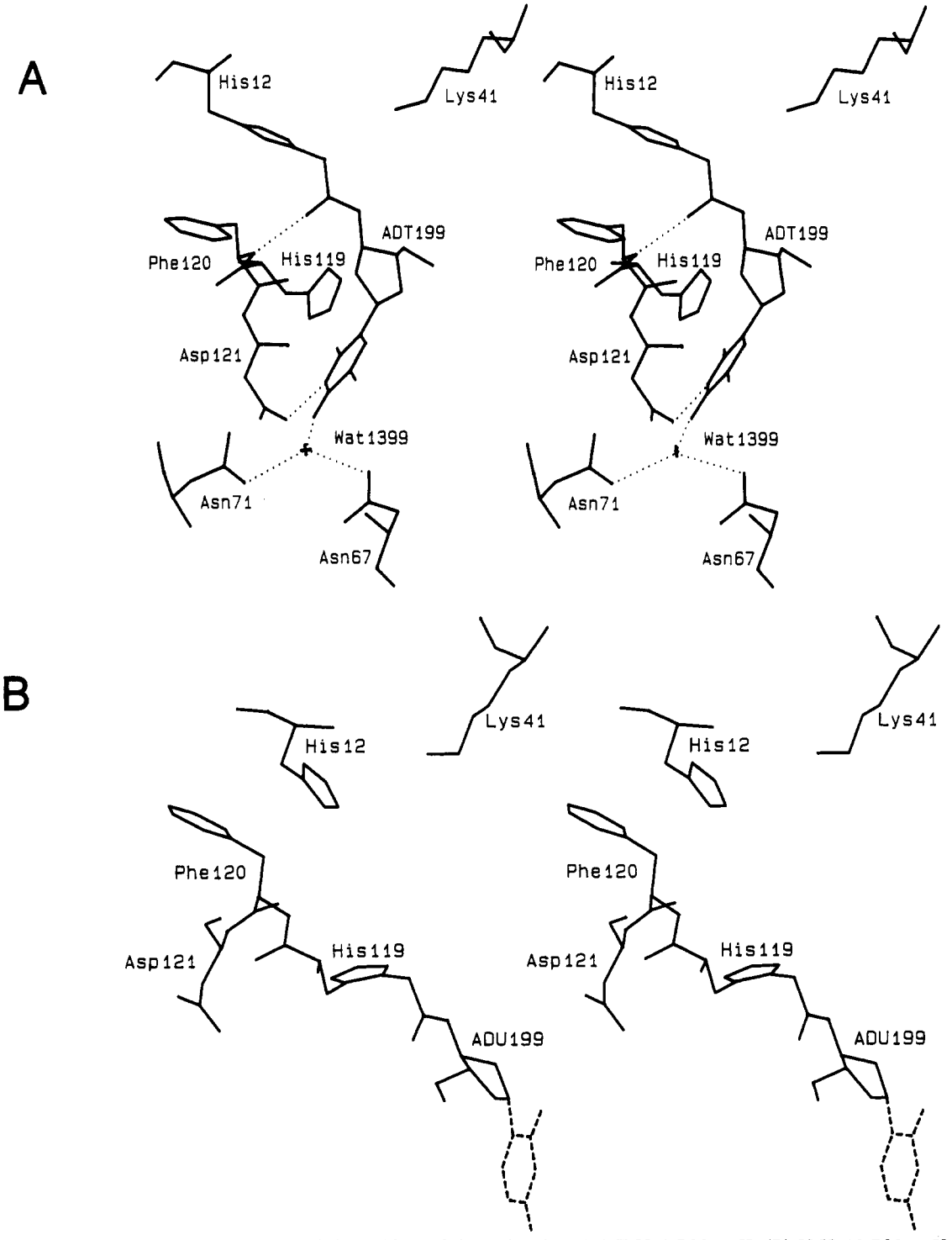

FIGURE 5: Interaction between the nucleosides and the residues of the active site: (A) T-H12-RNase II; (B) U-H119-RNase II (modeled part of the nucleoside dashed).

a certain residue in one molecule involved in a certain intermolecular hydrogen bond forms a different or no contact in the other molecule in the asymmetric unit. The only intermolecular hydrogen bond present in both molecules in the asymmetric unit is made between O_{ϵ_1} of Gln69 of one molecule and the carbonyl oxygen of Tyr76 of the symmetry mate of the other crystallographically independent molecule. This difference between the crystallographic environments of the molecules in the asymmetric unit is probably one of the causes for the differences in atomic positions and temperature factors between them.

The general features of the crystal packing of U-H119-RNase are similar to those of T-H12-RNase. There is, however, one major difference, namely, the possible involvement, in the case of U-H119-RNase, of the deoxyuridine substituent in forming intermolecular contacts between symmetry-related molecules. Thus, O4 of deoxyuridine in molecule I can form a hydrogen bond to O_{γ_1} of Thr87 of the symmetry mate of molecule II, while corresponding O4 of deoxyuridine in molecule II is probably hydrogen bonded to N_ϵ of Arg33 in the symmetry mate of molecule I. These assignments involve parts of the model which are not well seen in the electron density map and should be treated with caution.

(*e*) *Solvent Molecules.* At the end of the refinement of T-H12-RNase 246 solvent peaks were identified in the asymmetric unit, and all were treated as water oxygens. Out of

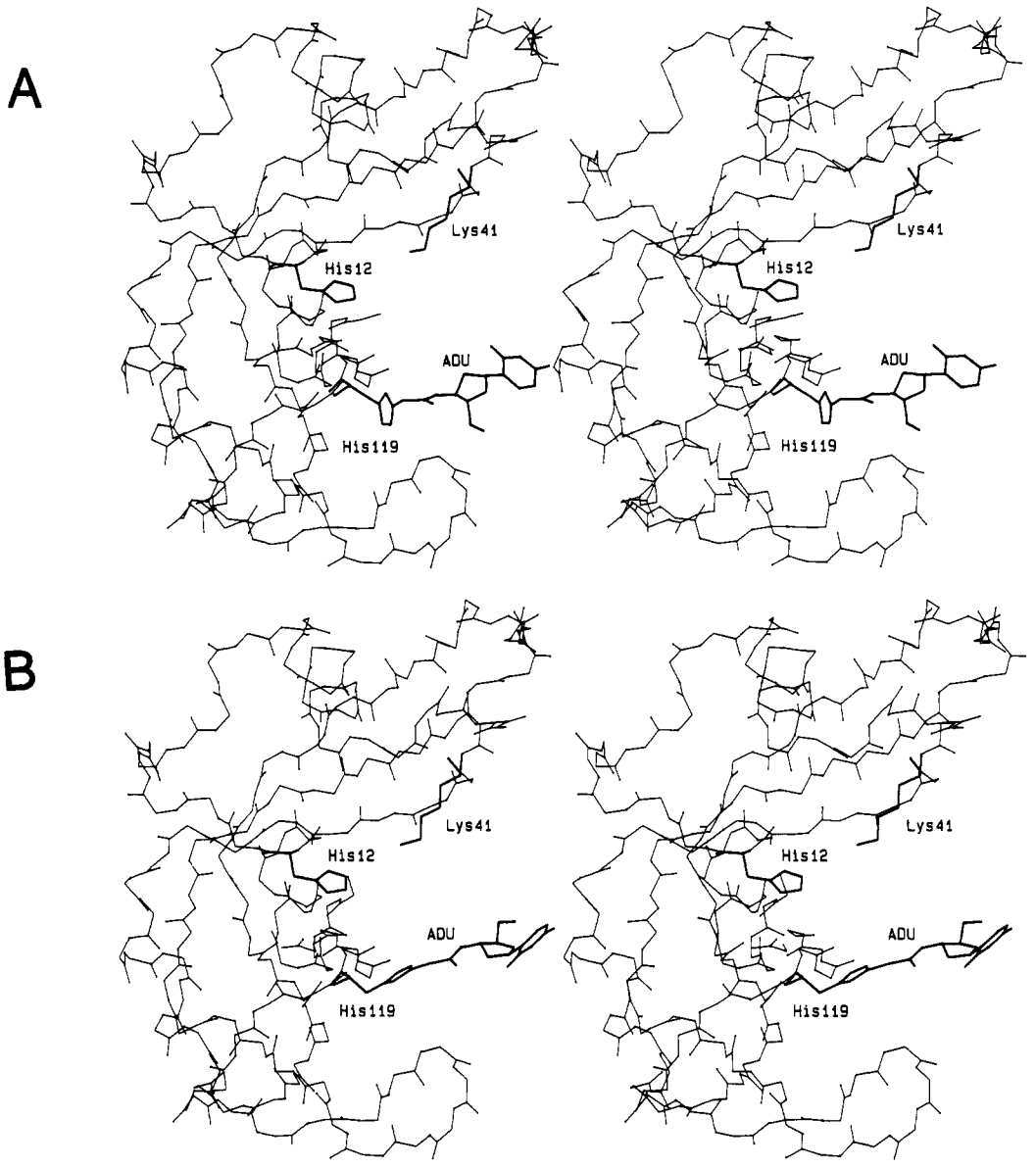

FIGURE 6: Modeling of nucleosides bound to alternate positions on His119: (A) Model for RNase with deoxyuridine covalently bound to $N_{\epsilon 2}$ of His119, the latter in the conformation found in the crystal structure of T-H12-RNase (compare with Figure 2A); (B) same as (A) but with His119 in the conformation found in the crystal structure of U-H119-RNase (compare with Figure 2B).

these, 4 belong to both independent molecules in the asymmetric molecules, forming bridges between them, 109 are associated with molecule I, and 133 are associated with molecule II. A total of 31 solvents in the asymmetric unit form intermolecular hydrogen bonds between residues belonging to symmetry-related molecules of T-H12-RNase.

No solvent peaks could positively be identified as sulfate ions. However, Wat1001 may be a likely candidate for a sulfate ion on the basis of O–O and N–O distances.

Discussion

The two structures described here differ in the degree of detail of the nucleoside substituents visible in electron density maps, while their protein structure is virtually identical (with the major exception of the positions of His119). For these reasons, only the structure of T-H12-RNase was discussed in detail in the previous section as far as crystal packing, solvent structure, and differences with the native enzyme are concerned. One problem encountered by us is that while the whole nucleoside was clearly visible in the electron density map of T-H12-RNase, only a small part of it was seen in U-H119-RNase, the sugar and the base being disordered. Our interpretation of these results must take into account this important difference.

Table V: NH Phe120–Ligand Oxygen Contacts in RNase A Derivatives

complex	N Phe120–O distance (Å)	N–X···O angle (deg) (X = H or D)	X–O distance (Å)
T-H12-RNase	2.62	175	1.62
PO_4–RNase A[a]	2.84	166	1.84
UpcA–RNase S[b]	3.03	155	2.10

[a] Data taken from the joint X-ray/neutron diffraction study of Wlodawer and Sjölin (1983). [b] Data taken from Richards and Wyckoff (1973).

The O8′ atom of the nucleoside in T-H12-RNase occupies a region of the active site where the O3 atom of the phosphate ligand residues in crystals of RNase A (Wlodawer & Sjölin, 1983) and where the O3P1 atom of UpcA is found in crystals of the UpcA–RNase S complex (Richards & Wyckoff, 1973). The O8′ atom is 2.62 Å from the backbone N of Phe120, and the N–H···O angle is 175° (Table V). This strong H-bond contact effectively immobilizes the aminoacyl link, minimizing

rotation about C9′–C8′. Major motions in the nucleoside moiety are limited, therefore, to rotations about N3′–C3′ and the glycosidic bond, N1–C1′. Model building studies reveal that rotations about these bonds are not capable of placing the pyrimidine base in the B1 site even when a variety of sugar ring puckers are imposed on the nucleoside structure.

The analysis of the aminoacyl linkage region of T-H12-RNase suggests structures for earlier alkylation products such as [$N^{\epsilon 2}$-[(carboxamido)methyl]histidine-12]RNase A (Fruchter & Crestfield, 1967) and [$N^{\epsilon 2}$-(carboxymethyl)-histidine-12]RNase A (Crestfield et al., 1963). In both structures the carboxamido and carboxyl oxygen could hydrogen bond to the NH of Phe120 to act as a bridge across the active site. Further stabilizing contacts might arise between the imidazole side chain of His119 and the NH_2 group of the carboxamido residue or the alternate oxygen of the carboxyl group.

While the nucleoside moiety in T-H12-RNase is partially disordered with one major conformer, the uridine portion of U-H119-RNase is totally disordered. This results primarily from several features of the U-H119-RNase structure which are different from the T-H12-RNase structure in the aminoacyl linkage region. Primarily, the O8′ carbonyl oxygen is not hydrogen bonded to any proton donor on the enzyme surface, allowing considerable rotation about C9′–C8′. Second, the direction of the aminoacyl linkage region suggests that the sugar and base moieties of the uridine portion of the molecule are in regions where they would be unable to make stabilizing contacts with groups on the enzyme. Nevertheless, the partial structure of U-H119-RNase suggests a structural pathway for bis-alkylation of His119. Assuming that 3′-(bromoacetamido)-3′-deoxyuridine alkylates His119 only subsequent to binding to the B_1–R_1–p_1 site, rotational motions about C_α–C_β and C_β–C_γ in the His119 side chain would allow an additional bromoacetamido nucleoside to bind in B_1–R_1–p_1 and at the same time position N_{ϵ_2} of His119 in an orientation favorable for alkylation.

The different conformation of the substituted catalytic site may provide an explanation for the difference in the enzymatic activity between the two modified forms of RNase. In the case of T-H12-RNase, the deoxythymidine sits across the active site of RNase; therefore, it not only inhibits the capability of His12 to participate in the proton shuttle necessary for the hydrolysis of the phosphodiester bond in RNA, but it also physically prevents the approach of the substrate to the active site. In U-H119-RNase, the deoxyuridine, while still interfering with the proton shuttle, leaves the active site partially open to approach of the substrate.

On the basis of the crystal structure of T-H12-RNase and that of U-H119-RNase, where the deoxyuridine is covalently bound to N_{δ_1} of His119, we built models for RNase substituted at N_{ϵ_2} of His119, with the imidazole ring occupying both the position observed in U-H119-RNase and that found in T-H12-RNase. The orientation of the substituent was chosen so as to avoid close contacts with the atoms of RNase. For each position of His119, one of the possible models of U-H119-RNase is shown in Figure 6. As can be seen, in neither case would substitution at N_{ϵ_2} of His119 cause the histidine–deoxyuridine moiety to block the access to the catalytic site; by analogy with T-H12-RNase, this would result in retention of some residual enzymatic activity. Moreover, since according to these models substitution at N_{ϵ_2} can occur with His119 adopting both conformations observed in the crystal structures of T-H12-RNase and of U-H119-RNase, respectively, one may assume that in this case the histidine–deoxyuridine moiety has a higher flexibility than in the case of substitution at N_{δ_1}, where His119 adopts only one conformation.

The fact that the modifications in which RNase is substituted at His119 exhibit some residual enzymatic activity suggests that monosubstitution of His119 does not completely inhibit the capability of this residue to participate in the proton shuttle and that proton transfer can occur from either N_{δ_1} or N_{ϵ_2}. This would be in agreement with the side-chain mobility of His119 observed in the crystal structure of native RNase A by Borkakoti et al. (1982), who reported occupancies of the two sites for the imidazole ring of His119 of 0.2 and 0.8, respectively. These numbers are similar to the residual enzymatic activities of the two deoxyuridine-monosubstituted forms of RNase: 1% for substitution at N_{δ_1} and 5% for substitution at N_{ϵ_2} (Hummel et al., 1987). This seems to confirm the assumption that the mobility of His119 is reflected in the mode of catalysis.

Acknowledgments

We thank Dr. Andrew Howard of Genex Corp. for helpful discussions concerning the data processing and Susan Kelly for preparing the manuscript. The contents of this paper do not necessarily reflect the views or policies of the Department of Health and Human Services or the National Institute of Standards and Technology. Certain commercial equipment, instruments, and materials are identified in this paper in order to specify the experimental procedure. Such identification does not imply recommendation or endorsement by the National Institute of Standards and Technology or the National Cancer Institute, nor does it imply that the materials or equipment identified are necessarily the best available for the purpose.

Registry No. 3′-(Bromoacetamido)-3′-deoxythymidine, 105663-65-8; 3′-(bromoacetamido)-3′-deoxyuridine, 105639-33-6.

References

Borkakoti, N. (1983) *Eur. J. Biochem. 132*, 89–94.

Borkakoti, N., Moss, D. S., & Palmer, R. A. (1982) *Acta Crystallogr., Sect. B 38*, 2210–2217.

Borkakoti, N., Palmer, R. A., Haneef, I., & Moss, D. S. (1983) *J. Mol. Biol. 169*, 743–755.

Campbell, R. L., & Petsko, G. A. (1987) *Biochemistry 26*, 8579–8584.

Carty, R. P., & Hirs, C. H. W. (1968) *J. Biol. Chem. 243*, 5244–5253.

Crestfield, A. M., Stein, W. H., & Moore, S. (1963) *J. Biol. Chem. 238*, 2413–2421.

Crowther, R. A. (1972) in *The Molecular Replacement Method* (Rossman, M. G., Ed.) pp 173–178, Gordon and Breach, New York.

Crowther, R. A., & Blow, D. W. (1967) *Acta Crystallogr. 23*, 544–549.

Finzel, B. C. (1987) *J. Appl. Crystallogr. 20*, 53–55.

Fitzgerald, P. M. D. (1988) *J. Appl. Crystallogr. 21*, 273–278.

Fruchter, R. G., & Crestfield, A. M. (1967) *J. Biol. Chem. 242*, 5807–5813.

Hendrickson, W. A. (1985) *Methods Enzymol. 115*, 252–270.

Howard, A. J., Gilliland, G. L., Finzel, B. C., Poulos, T. L., Ohlendorf, D. H., & Salemme, F. R. (1987) *J. Appl. Crystallogr. 20*, 383–387.

Hummel, C. F., Pincus, M. R., Brandt-Rauf, P. H., Frei, G. M., & Carty, R. P. (1987) *Biochemistry 26*, 135–146.

Lin, S. H., Konishi, Y., Denton, M. E., & Scheraga, H. A. (1984) *Biochemistry 23*, 5504–5512.

Pincus, M. R., Le Thi, L., & Carty, R. P. (1975) *Biochemistry 14*, 3653–3661.

Richards, F. M., & Wyckoff, H. W. (1973) in *Atlas of Mo-*

lecular Structure in Biology, Vol. I, Ribonuclease S (Phillips, D. C., & Richards, F. M., Eds.) Clarendon, Oxford.
Saenger, W. (1973) *Angew. Chem., Int. Ed. Engl. 12*, 591–601.
Sheriff, S. (1987) *J. Appl. Crystallogr. 20*, 55–57.
Svensson, L. A., Sjölin, L., Gilliland, G., Finzel, B. C., & Wlodawer, A. (1987) *Proteins 1*, 370–375.
Ward, K. B., Wishner, B. C., Lattman, E. E., & Love, M. E. (1975) *J. Mol. Biol. 180*, 301–329.
Williams, R. L., Greene, S. M., & McPherson, A. (1987) *J. Biol. Chem. 262*, 16020–16031.
Wlodawer, A. (1985) in *Biological Macromolecules and Assemblies*, Vol. II, Nucleic Acids and Interactive Proteins (Jurnak & McPherson, Eds.) pp 395–439, Wiley, New York.
Wlodawer, A., & Sjölin, L. (1983) *Biochemistry 22*, 2720–2727.
Wlodawer, A., Svensson, L. A., Sjölin, L., & Gilliland, G. L. (1988) *Biochemistry 27*, 2705–2717.

Determinants of Visual Pigment Absorbance: Role of Charged Amino Acids in the Putative Transmembrane Segments†

Jeremy Nathans

Howard Hughes Medical Institute, Department of Molecular Biology and Genetics, and Department of Neuroscience, Johns Hopkins University School of Medicine, 725 North Wolfe Street, Baltimore, Maryland 21205

Received August 14, 1989; Revised Manuscript Received September 14, 1989

ABSTRACT: I have investigated the effect on bovine rhodopsin's absorbance spectrum of charged amino acid changes in the putative membrane-spanning regions. A total of 14 site-directed mutants were constructed at 6 amino acid positions: 83, 86, 122, 134, 135, and 211. Two of these positions are occupied by charged amino acids that are conserved in all four human visual pigments (positions 134 and 135). In the four variable positions, single and double mutants were constructed to reproduce the intramembrane distribution of charged amino acids predicted for each human cone pigment. Following solubilization in digitonin and reconstitution with 11-*cis*-retinal, the photobleaching difference spectrum of each pigment was determined in the presence of hydroxylamine. The absorbance spectra of the mutant pigments are all surprisingly close to that of native bovine rhodopsin (λ_{max} = 498 nm), ruling out a significant role for these residues in spectral tuning.

Visual pigments are the light-absorbing proteins in the retina responsible for initiating visual excitation. Each consists of a protein, opsin, bound via a protonated Schiff's base to a small chromophore, 11-*cis*-retinal (or in some instances a closely related retinal). The absorbance spectra of a large number of visual pigments have been determined, and these spectra have in common a broad bell shape, closely resembling the shape of a protonated Schiff's base of retinal free in solution. They differ from one another and from the free chromophore in their positions along the wavelength axis: points of maximal absorbance have been found throughout the visible range, from far-red to near-ultraviolet. Presumably, amino acid sequence differences among the visual pigments determine their distinctive absorbance spectra.

The experiments reported here are aimed at determining the role of particular amino acids in spectral tuning. Recently, the amino acid sequences of a number of visual pigments have been determined, including bovine (Ovchinnikov et al., 1983; Hargrave et al., 1983; Nathans & Hogness, 1983), chicken (Takao et al., 1988), human (Nathans & Hogness, 1984), mouse (Baehr et al., 1988), octopus (Ovchinnikov et al., 1988), and *Drosophila* (O'Tousa et al., 1985; Zuker et al., 1985, 1987; Cowman et al., 1986; Montell et al., 1987) rhodopsins and the three human cone pigments (Nathans et al., 1986). These sequences define a family of homologous proteins and provide a data base to guide future experiments. It is reasonable to suppose that highly conserved properties such as efficient isomerization, transducin activation, and phosphorylation will be reflected in the conservation of single amino acids or protein domains. Conversely, those properties that differ between pigments, for example, the absorbance spectrum, will be reflected in protein sequence differences. This simple approach has been used effectively in many systems. To cite just one example, in the study of immunoglobulins, the regions which form the ligand binding pocket were correctly predicted from sequence comparisons before they were visualized by X-ray crystallographic studies (Wu & Kabat, 1970; Amzel et al., 1974).

The starting point for the experiments presented here is the spectral absorbance and amino acid sequence data for the four human visual pigments. Human rhodopsin, which mediates vision in dim light, peaks at 493–497 nm (Crescitelli & Dartnall, 1953; Wald & Brown, 1958); the three human cone pigments, which mediate color vision, peak at approximately 420, 530, and 560 nm [referred to as blue, green, and red pigments, respectively (Dartnall et al., 1983)]. Comparison of the red and green pigment amino acid sequences shows 96% identity whereas all other pairwise comparisons show approximately 40% identity (Nathans et al., 1986). The sequence differences define candidate amino acids that may be involved in spectral tuning.

All visual pigment sequences reveal seven predominantly hydrophobic stretches of amino acids. These are presumed to form a bundle of seven membrane-spanning α-helical segments, an arrangement consistent with protein modification experiments using water-soluble probes [see Nathans (1987) for a recent review]. 11-*cis*-Retinal is covalently attached to lysine-296 (in the bovine rhodopsin numbering system) in the center of the seventh hydrophobic stretch (Bownds, 1967;

† This research was supported by the National Eye Institute (NIH) and the Howard Hughes Medical Institute.

0006-2960/90/0429-937$02.50/0